Research Square

Preprints are preliminary reports that have not undergone peer review.
They should not be considered conclusive, used to inform clinical practice,
or referenced by the media as validated information.

Metagenome-guided discovery of L-arabinose isomerases from the goat rumen microbiome for whole-cell cascade production of L-ribose

Fengzhen Chen
Fuzhou University
Jiayun Ding
Fuzhou University
Zhanying Yang
Pucheng Chai Tai Biochemistry Co., Ltd.
Lulong Zhong
Ningde Institute of Agricultural Sciences
Xian'ai Shi
Fuzhou University
Guozeng Wang
wanggz@fzu.edu.cn

Fuzhou University

Research Article

Keywords: L-Ribose, L-Arabinose isomerase, D-lyxose isomerase, Rumen metagenome, Whole-cell cascade biocatalysis

Posted Date: November 23rd, 2026

DOI: https://doi.org/10.21203/rs.3.rs-11686227/v1

License: This work is licensed under a Creative Commons Attribution 4.0 International License. Read Full License

Additional Declarations: No competing interests reported.

Abstract

L-Ribose is a high-value rare sugar and an important intermediate for the synthesis of several antiviral and antitumor L-nucleosides. This study used a metagenome-guided strategy to discover L-arabinose isomerases from the Boer goat rumen microbiome and to establish a whole-cell cascade for L-ribose production. Seventy-nine complete candidate genes were identified, and nine representative genes were selected for experimental validation. Eight candidates were successfully cloned and expressed, and GR-AI2, GR-AI6, GR-AI8, and GR-AI9 showed relatively high L-arabinose isomerization activity. The four enzymes exhibited optimal temperatures of 50–55°C and pH optima of 7.0–7.5. Their apparent K_m values for L-arabinose were 710.8, 72.99, 209.20, and 139.40 mM, respectively, and the corresponding V_{max} values were 8.08, 10.37, 40.62, and 76.12 μmol min^{-1} mg^{-1}. GR-AI8 and GR-AI9 were separately co-expressed with the rumen-derived D-lyxose isomerase GR-LI1 to construct resting-cell cascades that converted L-arabinose to L-ribose. At 50°C, pH 7.0, 1 mM Co^{2+}, and 220 rpm, the GR-AI9/GR-LI1 system produced 18.80, 54.51, and 78.97 g/L L-ribose from 100, 300, and 500 g/L L-arabinose, corresponding to product yields of 18.80%, 18.17%, and 15.79%, respectively. These results expand the functional L-arabinose isomerase resource available from the rumen metagenome and identify GR-AI9/GR-LI1 as a promising whole-cell cascade for further process intensification under high substrate loading.

1. Introduction

Rare sugars are low-abundance monosaccharides and their derivatives that have attracted considerable interest for applications in food, nutrition, and pharmaceutical synthesis (1–3). L-Ribose is a high-value rare pentose and an important intermediate for several antiviral and antitumor L-nucleosides (4–6). Greener and more efficient routes for L-ribose production are therefore of continued scientific and industrial interest (7, 8).

L-Ribose is mainly produced by chemical synthesis or biotransformation (6, 9–11). Chemical routes typically involve multistep stereochemical conversion of pentoses or carbon-chain shortening of hexoses (10, 11), whereas enzymatic routes offer milder conditions, higher selectivity, and lower environmental burden. Izumoring established a general framework for rare-sugar synthesis through combinations of isomerization, epimerization, and redox reactions (12, 13). Biosynthetic routes to L-ribose commonly start from L-arabinose or ribitol (14). L-Arabinose is particularly attractive as a readily available starting material, and an immobilized recombinant *Escherichia coli* system co-expressing L-arabinose isomerase and mannose-6-phosphate isomerase has achieved approximately 33% product yield (15). However, enzyme performance, reaction equilibrium, and potential reductions in activity at high substrate concentrations remain challenges, highlighting the need for isomerases with improved catalytic properties and substrate tolerance (16).

L-Arabinose isomerase (L-AIase; EC 5.3.1.4) catalyzes the reversible conversion of L-arabinose to L-ribulose and is the first key enzyme in L-arabinose-based L-ribose cascades. Many L-AIases also catalyze D-galactose isomerization to D-tagatose and are therefore relevant to rare-sugar biomanufacturing (17). Early biochemical studies established the L-arabinose-to-L-ribulose isomerization reaction (18), and enzymes from diverse microorganisms have subsequently been characterized, particularly those from lactic acid bacteria and bifidobacteria (19–23). More recently, L-AIases from *Arthrobacter psychrolactophilus* B7 and a bovine-rumen metagenome have further expanded the available enzyme repertoire (24, 25). Nevertheless, improved enzyme performance and effective operation at high substrate loading remain desirable.

Metagenomics enables direct enzyme discovery from uncultivated microorganisms and has been widely applied to complex environments (26–28). The rumen microbiome is particularly rich in carbohydrate-active microorganisms and represents a promising source of isomerases. Xylose isomerases have been recovered from goat and bovine rumen microbiomes and related microorganisms (29–31), and a linoleic acid isomerase has been cloned from a bovine-rumen isolate (32). A previous study identified 61 arabinose-isomerase-related gene fragments from sheep-rumen microorganisms, with many assigned to *Prevotella* (33). Our laboratory has also identified several D-lyxose isomerases from a goat-rumen metagenome (34). However, systematic functional characterization of rumen-derived L-AIases and their application in L-ribose synthesis remain limited.

In this study, a Boer goat rumen metagenome was mined for L-AIase candidates, followed by phylogenetic analysis, heterologous expression, activity screening, and biochemical characterization. GR-AI8 and GR-AI9 were further co-expressed individually with the previously obtained D-lyxose isomerase GR-LI1 to construct whole-cell cascades for L-ribose production, and their performance was evaluated at increasing L-arabinose concentrations.

2. Materials and methods

2.1. Materials, strains, and expression vector

Escherichia coli BL21(DE3) and pET-28a(+) were obtained from Invitrogen (Carlsbad, CA, USA) and Novagen (Schwalbach, Germany), respectively. Tryptone and yeast extract were purchased from OXOID (Hampshire, UK); the ClonExpress II One Step Cloning Kit from Vazyme (Nanjing, China); DNA purification and plasmid extraction kits from Omega (Norcross, GA, USA); IPTG and kanamycin sulfate from Takara (Otsu, Japan); and Ni-NTA agarose from Qiagen (Valencia, CA, USA). D-Galactose, D-ribose, D-glucose, D-mannose, D-xylose, protein molecular-mass markers, and DNA markers were obtained from Sangon Biotech (Shanghai, China), and L-arabinose from Solarbio (China). Ni-NTA agarose was used for affinity purification of His_6-tagged recombinant proteins. Unless otherwise specified, all other chemicals were of analytical grade.

2.2. Identification and sequence analysis of L-arabinose isomerases from the goat-rumen metagenome

Potential L-AIase-encoding genes were first retrieved from the goat-rumen metagenomic dataset (34) according to conserved domain features of known L-AIases. Predicted proteins were compared with reported homologs using NCBI BLAST to assess the reliability of functional annotation. A phylogenetic tree was then constructed in MEGA 5.0 and visualized with EvolView to examine evolutionary relationships and source diversity. To compare sequence conservation among candidates, multiple sequence alignment of candidate L-AIases and biochemically characterized homologs was performed with Clustal W. BioEdit version 7.2.5 was used to generate sequence-identity matrices, which were visualized as heat maps using Origin 2020.

2.3. Expression and purification of recombinant L-arabinose isomerases

Nine representative L-AIase genes, designated GR-AI1 to GR-AI9, were selected from the rumen metagenome. Target genes were amplified from rumen metagenomic DNA using gene-specific primers (Table S1). GR-AI4 did not yield the expected amplicon; the remaining eight genes were recovered and assembled into pET-28a(+)

using the ClonExpress II One Step Cloning Kit. Recombinant plasmids were first transformed into *E. coli* TOP10 and verified by colony PCR and sequencing, and confirmed plasmids were then transformed into *E. coli* BL21(DE3) for protein expression. Expression cultures were inoculated at 1% (v/v) into LB medium and cultivated at 37°C and 200 rpm to an OD_{600} of approximately 0.5. Expression was induced with 0.5 mM IPTG at 20°C and 200 rpm for 16 h. Cells were harvested at 10,000 × g for 5 min at 4°C, washed twice with 20 mM Tris-HCl (pH 7.6), resuspended, and disrupted by sonication at 200 W using 2-s pulses separated by 5-s intervals for a total of 20 min. Cell debris was removed by centrifugation at 12,000 × g for 10 min at 4°C. Recombinant proteins were purified by Ni^{2+}-affinity chromatography using a 20–600 mM imidazole elution gradient, and expression and purification were assessed by 10% SDS–PAGE. Protein concentration was determined by the Bradford method using bovine serum albumin as the standard (35).

2.4. L-Arabinose isomerase activity assay

L-AIase activity was evaluated by quantifying the formation of L-ribulose from L-arabinose. The standard reaction mixture (200 μL) contained 50 mM L-arabinose, 1.0 mM $CoCl_2$, 20 μL enzyme solution, and McIlvaine buffer (pH 7.0) to volume. Reactions were incubated at 50°C for 10 min and immediately cooled in an ice bath for 5 min. A 30-μL aliquot was mixed with 750 μL color reagent containing 0.12% carbazole in ethanol, 1.5% cysteine hydrochloride, and 70% sulfuric acid at a volume ratio of 1:1:25. After color development for 10 min at room temperature, absorbance was recorded at 540 nm and used to calculate L-ribulose formation (36). One unit of activity was defined as the amount of enzyme required to produce 1 μmol L-ribulose per minute under the specified conditions.

2.5. Biochemical properties and kinetic parameters of recombinant L-arabinose isomerases

Using the standard assay as a basis, the effects of pH (5.0–11.0), temperature (30–70°C), metal ions, and substrate identity were evaluated for the four active recombinant L-AIases. Substrate tests included L-arabinose, D-galactose, D-ribose, D-glucose, D-mannose, and D-xylose. Thermal stability was assessed after incubation at selected temperatures for 0–60 min. Kinetic parameters were determined from initial rates measured over a range of L-arabinose concentrations under the optimal conditions for each enzyme and were fitted to the Michaelis-Menten equation to obtain K_m and V_{max}. Detailed procedures are provided in the Supplementary Methods.

2.6. Construction of L-AIase/D-lyxose isomerase co-expression systems and L-ribose production

GR-AI8 and GR-AI9 were amplified from pET-28a-GR-AI8 and pET-28a-GR-AI9, respectively, and each gene was assembled with the previously constructed pETDuet-GR-LI1 plasmid carrying the D-lyxose isomerase gene GR-LI1 (34). Recombinant plasmids enabling co-expression of L-AIase and D-lyxose isomerase were verified by transformation, screening, and sequencing before use in whole-cell cascade reactions. Co-expression cultures were grown to an OD_{600} of approximately 0.6 and induced with 0.5 mM IPTG for 14–16 h at 20°C. Cells were harvested at 10,000 × g for 5 min at 4°C, washed twice with 20 mM Tris-HCl (pH 7.6), and used as resting cells. The effects of pH 6.0–9.0, temperature 40–70°C, and metal ions on the relative activities of L-AIase and D-LI in the co-expression systems were first evaluated. Resting-cell concentrations of 10, 20, 30, 40, and 50 g wet cell weight/L were then tested for 15 min to compare cell loading. Cascade reactions were subsequently performed

using initial L-arabinose concentrations of 100, 300, and 500 g/L at the selected cell concentrations. Samples were analyzed by HPLC to quantify L-ribose production as described in Section 2.7.

2.7. HPLC analysis of L-arabinose, L-ribulose, and L-ribose

L-Arabinose, L-ribulose, and L-ribose were analyzed using an HPLC system equipped with a refractive index detector. Separation was performed using a Carbomix Ca carbohydrate-analysis column (Sepax Technologies, USA; 5 μm, 8% cross-linking, 7.8 × 300 mm). Ultrapure water, filtered through a 0.22-μm membrane and thoroughly degassed, was used as the mobile phase at 0.6 mL/min. The column temperature was maintained at 80°C, and the injection volume was 10 μL. Quantitative analysis of L-arabinose and L-ribose was performed using their respective calibration curves.

2.8. Data submission

All L-arabinose isomerase genes obtained from the goat rumen metagenome in this study were submitted to the NCBI database, and their accession numbers are QB146167–QB146245.

3. Results and discussion

3.1. Phylogenetic and sequence diversity of rumen-metagenome L-arabinose isomerases

Functional annotation and homology searches of the Boer goat rumen metagenome generated in our previous study (34) identified 79 complete candidate genes with substantial similarity to known L-arabinose isomerases (L-AIases). The corresponding proteins were predominantly approximately 500 amino acids in length, consistent with the typical size of this enzyme family. To determine how these candidates were related to one another and to assess the extent of sequence diversity within the metagenomic pool, phylogenetic and comparative sequence analyses were subsequently performed.

Phylogenetic analysis resolved the 79 candidate L-AIases into seven major groups (Fig. 1), revealing substantial diversification within the candidate set. To relate this phylogenetic structure to the microbial origin of the sequences, the taxonomic assignments derived from the original metagenomic annotations were further examined. The candidates were affiliated with Oscillospiraceae, Bacteroidales, Bacteroidaceae, *Prevotella*, Lachnospiraceae, and Clostridia. *Prevotella*-associated sequences accounted for 26.6% of the total, whereas sequences affiliated with *Prevotella*, Lachnospiraceae, Oscillospiraceae, and Clostridia collectively represented approximately 69.62% of the dataset. Notably, sequences with different taxonomic affiliations were distributed across multiple phylogenetic branches rather than forming strictly taxon-specific clusters, suggesting that the observed diversity extended beyond differences in microbial origin alone.

Because phylogenetic grouping provides only a relative measure of evolutionary relatedness, the degree of sequence divergence was further quantified by BLASTp comparison against homologous proteins deposited in GenBank. The candidate proteins shared approximately 68%–99% amino-acid identity with their closest database homologs (Fig. S1). Approximately 68% of the candidates exhibited > 90% identity, nearly one-quarter showed 80%–90% identity, and a smaller subset showed 68%–80% identity. Thus, although most candidates

were closely related to previously annotated L-AIase homologs, a distinct fraction displayed appreciably lower sequence identity and therefore represented the more divergent portion of the sequence pool.

The phylogenetic distribution showed that Groups 3, 4, and 7 were the three largest groups, together accounting for 78.48% of all candidate sequences. To examine sequence-identity patterns across the complete candidate set, pairwise amino acid sequence identity heat maps were generated for sequences assigned to all seven phylogenetic groups (Fig. S2). For clarity of presentation, Groups 3, 4, and 7 were displayed individually in Fig. S2a, c, and d, respectively, whereas sequences assigned to Groups 1, 2, 5, and 6 were combined in a single heat map in Fig. S2b. These four groups collectively accounted for the remaining 21.52% of candidates; their combined presentation provides a compact overview of their sequence-identity patterns without altering their distinct phylogenetic assignments. Group 3 contained sequences annotated as *Prevotella* sp., Oscillospiraceae bacterium, and Lachnospiraceae bacterium, whereas Group 4 was mainly composed of Lachnospiraceae bacterium- and *Prevotella* sp.-associated sequences. Group 7, which alone represented approximately 35% of all candidates, included sequences annotated as Oscillospiraceae bacterium, *Prevotella* sp., and Clostridia bacterium. The heat maps revealed differences in sequence conservation among the groups. Group 7 was comparatively more conserved, whereas greater sequence divergence was observed in several other groups. Taken together, the phylogenetic distribution, taxonomic composition, and pairwise sequence-identity patterns demonstrated substantial sequence heterogeneity among the rumen-derived L-AIase candidates.

On the basis of this combined analysis, nine genes representing different phylogenetic positions and levels of sequence divergence were selected for functional characterization: JLW_83464 (GR-AI1), JLW_75439 (GR-AI2), JLW_97784 (GR-AI3), JLW_137457 (GR-AI4), JLW_302579 (GR-AI5), JLW_392531 (GR-AI6), JLW_1374526 (GR-AI7), JLW_1230584 (GR-AI8), and JLW_1087962 (GR-AI9). The encoded proteins contained 476–527 amino acids and shared 74%–96% identity with their closest GenBank homologs (Table S2). GR-AI4 did not yield the expected PCR product, whereas the remaining eight genes were successfully amplified and used for subsequent cloning, heterologous expression, and activity screening.

3.2. Heterologous expression and purification of GR-AI2, GR-AI6, GR-AI8, and GR-AI9

Activity screening of the eight successfully cloned and expressed candidates revealed marked differences in L-arabinose isomerization activity (Fig. S3). Among them, GR-AI2, GR-AI6, GR-AI8, and GR-AI9 exhibited relatively high activity, whereas GR-AI1 showed only weak activity and no clear activity was detected for GR-AI3, GR-AI5, or GR-AI7 under the assay conditions. Based on these results, the four most active enzymes were selected for purification and subsequent biochemical characterization.

SDS–PAGE analysis of the purified proteins showed prominent bands within the expected molecular-mass range, in agreement with the calculated molecular masses of 54.16, 53.48, 53.80, and 53.33 kDa for GR-AI2, GR-AI6, GR-AI8, and GR-AI9, respectively (Fig. S4). Following Ni^{2+}-affinity chromatography, the corresponding target bands were markedly enriched, with a substantial reduction in contaminating proteins, confirming successful purification of the recombinant enzymes.

3.3. Biochemical and kinetic properties of recombinant L-arabinose isomerases

All four recombinant L-AIases exhibited optimal activities under neutral to slightly alkaline conditions, with apparent pH optima ranging from 7.0 to 7.5 (Fig. 2). GR-AI2 and GR-AI8 showed their highest activities at approximately pH 7.0, whereas GR-AI6 and GR-AI9 exhibited optimal activities at approximately pH 7.5. Notably, the four enzymes differed in their pH activity profiles. GR-AI2 showed a relatively narrow pH activity range, with a marked decrease in activity under alkaline conditions. In contrast, GR-AI6 and GR-AI8 retained substantial activity at pH 9.0, reaching approximately 59% and 74% of their respective maximum activities, respectively. GR-AI9 exhibited the broadest apparent pH tolerance, retaining approximately 95% of its maximum activity at pH 9.0. However, the activities of all four enzymes decreased substantially at pH 10.0 and above. These results indicate that the four L-AIases are predominantly neutral-pH-active enzymes, with GR-AI9 displaying particularly good activity retention under alkaline conditions.

The effects of temperature on the activities of the four recombinant L-AIases were investigated over a range of 30–70°C (Fig. 3). All four enzymes exhibited relatively high activities at 45–55°C, with optimal temperatures of 50°C for GR-AI2, GR-AI8, and GR-AI9, and 55°C for GR-AI6. However, their temperature-dependent activity profiles differed considerably. GR-AI2 showed a relatively narrow temperature activity profile, with its activity decreasing sharply above 55°C. GR-AI6 maintained approximately 65% of its maximum activity at 60°C. Notably, GR-AI8 exhibited a broader high-activity temperature range, retaining approximately 95% and 57% of its maximum activity at 55°C and 60°C, respectively. GR-AI9 also maintained high activity at 55°C (approximately 91%), but its activity declined sharply to approximately 28% at 60°C. Overall, GR-AI8 displayed the broadest temperature activity profile, whereas GR-AI6 showed the highest apparent optimal temperature among the four enzymes.

The thermal stability of the four recombinant L-AIases was further evaluated by measuring their residual activities after incubation at different temperatures for up to 60 min (Fig. S5). GR-AI2 exhibited relatively good stability at 35°C, retaining approximately 85% of its initial activity after 60 min, but its residual activity decreased markedly at higher temperatures. GR-AI6 showed the best thermal stability at moderately elevated temperatures, retaining approximately 84%, 72%, and 49% of its initial activity after 60 min of incubation at 45, 50, and 55°C, respectively. GR-AI8 exhibited excellent stability at 40°C, maintaining approximately 98% residual activity after 60 min, whereas its activity decreased to approximately 69%, 45%, and 21% following incubation at 45, 50, and 55°C, respectively. GR-AI9 showed a similar temperature-dependent stability profile, retaining approximately 88%, 74%, 48%, and 21% residual activity after 60 min at 40, 45, 50, and 55°C, respectively. Notably, GR-AI6 displayed a clear advantage over the other enzymes at 45–55°C, whereas GR-AI8 exhibited the highest stability at 40°C. Overall, GR-AI6 was the most thermostable enzyme under moderately elevated-temperature conditions, while GR-AI8 showed excellent stability at relatively mild temperatures.

The effects of divalent metal ions on catalytic activity were subsequently examined (Fig. S6). Co^{2+} resulted in the greatest enhancement of GR-AI2 and GR-AI6 activities, whereas Mn^{2+} produced the strongest stimulatory effect on GR-AI8 and GR-AI9. By contrast, Zn^{2+} and Cu^{2+} markedly inhibited the activities of most of the enzymes. Substrate-specificity assays showed that all four L-AIases displayed a clear preference for L-arabinose (Fig. S7). In particular, no detectable activity of GR-AI9 was observed toward D-galactose, D-ribose, or the other aldoses examined under the assay conditions, indicating relatively high substrate specificity toward L-arabinose.

Steady-state kinetic parameters were determined using L-arabinose as the substrate (Fig. S8). The apparent K_m values of GR-AI2, GR-AI6, GR-AI8, and GR-AI9 were 710.8, 72.99, 209.20, and 139.40 mM, respectively, and the corresponding V_{max} values were 8.08, 10.37, 40.62, and 76.12 μmol min^{-1} mg^{-1} (Table 1). Among the four enzymes, GR-AI6 exhibited the lowest apparent K_m, whereas GR-AI9 exhibited the highest V_{max}. Although GR-AI6 showed the lowest apparent K_m for L-arabinose, GR-AI8 and GR-AI9 exhibited higher maximum reaction velocities together with suitable pH and temperature characteristics and comparatively good stability. On this basis, GR-AI8 and GR-AI9 were selected for subsequent construction of co-expression systems with the D-lyxose isomerase GR-LI1.

Table 1
Major kinetic parameters and optimal reaction conditions of the four recombinant L-arabinose isomerases

Enzyme	Optimal temperature (°C)	Optimal pH	K_m (mM)	V_{max} (μmol min^{-1} mg^{-1})
GR-AI2	50	7.0	710.8	8.08
GR-AI6	55	7.5	72.99	10.37
GR-AI8	50	7.0	209.20	40.62
GR-AI9	50	7.5	139.40	76.12

To place the biochemical properties of the newly identified enzymes in the context of previously characterized L-AIases, representative enzymes reported in the literature were compared (Table 2). Substantial variation has been reported among L-AIases with respect to optimum temperature, optimum pH, metal-ion dependence, and kinetic parameters for L-arabinose (19–25). The four L-AIases characterized in the present study exhibited optimum temperatures of 50–55°C and pH optima of 7.0–7.5, representing a relatively consistent moderate-temperature and near-neutral catalytic profile.

Table 2
Comparison of the L-arabinose isomerases characterized in this study with representative reported enzymes

Enzyme/source	Optimal temperature (°C)	Optimal pH	Preferred metal ion(s)	K_m (mM)	Reference
GR-AI2	50	7.0	Co^{2+}	710.8	This study
GR-AI6	55	7.5	Co^{2+}	72.99	This study
GR-AI8	50	7.0	Mn^{2+}	209.20	This study
GR-AI9	50	7.5	Mn^{2+}	139.40	This study
B. longum	55	6.0–6.5	Mg^{2+}/Mn^{2+}	120	19
L. plantarum NC8	60	7.5	Co^{2+}/Mn^{2+}	43.4	20
L. sakei 23K	30–40	5.0–7.0	Mn^{2+}/Mg^{2+}	31.6	21
L. reuteri	65	6.0	Mn^{2+}/Co^{2+}	633	22
A. psychrolactophilus B7	60	7.0–7.5	Mn^{2+}	23.41	24
AraR (Bovine-rumen metagenome)	40–50	6.0–6.5	NR	5.552	25

NR, not reported.

With respect to apparent substrate affinity, the K_m value of GR-AI6 for L-arabinose (72.99 mM) was lower than those reported for the L-AIases from *B. longum* (120 mM) (19) and *L. reuteri* (633 mM) (22), but higher than those reported for *L. plantarum* NC8 (43.40 mM) (20) and *L. sakei* 23K (31.60 mM) (21). It was also higher than the values reported for the L-AIase from *A. psychrolactophilus* B7 (23.41 mM) (24) and the bovine-rumen-metagenome-derived AraR (5.55 mM) (25). Cross-study comparisons should be considered approximate because reaction conditions differ. Thus, the present enzymes were not distinguished by exceptionally low K_m values for L-arabinose. In contrast, GR-AI9 exhibited the highest V_{max} among the four enzymes (76.12 μmol min^{-1} mg^{-1}) and showed no detectable isomerization activity toward the other tested aldoses under the assay conditions.

Direct comparison of kinetic parameters among different L-AIases should, however, be interpreted cautiously because the assay temperature, pH, metal-ion composition, enzyme preparation, and kinetic analysis procedures differ among studies. In addition, some studies report kcat and k_{cat}/K_m rather than V_{max}, further limiting direct quantitative comparison. Taken together, the L-AIases identified in the present study are characterized by their rumen-metagenome origin, moderate optimum temperatures, near-neutral optimum pH, pronounced preference for L-arabinose, and suitability for integration with the GR-LI1-based whole-cell cascade, rather than by exceptionally low K_m values or unusually high thermostability.

3.4. Whole-cell L-AIase/D-lyxose isomerase cascades for L-ribose synthesis

GR-AI8/GR-LI1 and GR-AI9/GR-LI1 co-expression systems were constructed and evaluated as resting-cell biocatalysts for the one-pot cascade conversion of L-arabinose to L-ribose. Co-expression of the two enzymes was evaluated by SDS–PAGE (Fig. S9). For both recombinant strains, two prominent protein bands were observed in the induced samples, with apparent molecular masses of approximately 50 and 35 kDa. These bands corresponded to the purified GR-AI8 or GR-AI9 and GR-LI1, respectively. In contrast, the corresponding bands were not prominently detected in the uninduced samples. These results confirmed the successful co-expression of GR-AI8 and GR-LI1, as well as GR-AI9 and GR-LI1, in *Escherichia coli*, demonstrating that both enzyme pairs could be simultaneously expressed. To establish suitable operating conditions for the coupled reactions, the effects of temperature, pH, and divalent metal ions on the apparent whole-cell activities of L-AIase and D-LI were systematically investigated; the effect of resting-cell concentration on short-term L-ribose production was evaluated separately.

Both co-expression systems exhibited relatively high catalytic activities at approximately 60°C and retained substantial activity over the range of 50–70°C (Fig. 4a, c). Compared with the corresponding purified L-AIases, the whole-cell systems exhibited a broader temperature range over which catalytic activity was maintained, suggesting that cell-associated conditions may influence the apparent thermal response. Both systems also showed relatively high activities around pH 7.0 and retained substantial catalytic activity over pH 6.0–9.0, indicating compatibility of the two enzymatic steps under near-neutral reaction conditions (Fig. 4b, d).

The effects of divalent metal ions were subsequently examined because both L-AIase and D-LI require metal ions for catalytic activity. Mn^{2+} and Co^{2+} enhanced the apparent activities of both enzymatic steps, with Co^{2+} generally exerting the stronger stimulatory effect (Fig. 5a, c). In the GR-AI8/GR-LI1 system, for example, supplementation with Co^{2+} increased the apparent whole-cell L-AIase and D-LI activities by approximately 2.4- and 1.5-fold, respectively. Resting-cell concentration also affected short-term L-ribose production. The highest relative L-ribose production was observed at 20 g/L for GR-AI8/GR-LI1 and 40 g/L for GR-AI9/GR-LI1, whereas increasing the cell concentration to 50 g/L decreased the relative L-ribose concentration (Fig. 5b, d). Based on the combined effects of these parameters, 50°C, pH 7.0, 1 mM $CoCl_2$, and 220 rpm were selected for subsequent L-ribose production experiments.

Under the selected conditions, the effects of initial L-arabinose concentration on L-ribose production were evaluated using 20 g/L GR-AI8/GR-LI1 cells and 40 g/L GR-AI9/GR-LI1 cells. With 100 g/L L-arabinose, the GR-AI8/GR-LI1 system showed rapid product accumulation during the first 4 h, followed by a gradual decrease in the rate of L-ribose formation (Fig. 6a). The final L-ribose titer reached 17.85 g/L, corresponding to a yield of 17.85%. Increasing the initial L-arabinose concentration to 300 and 500 g/L increased the product titers to 45.84 and 55.13 g/L, respectively, whereas the corresponding yields decreased to 15.28% and 11.03%. Thus, although increasing substrate loading enhanced the final L-ribose titer, the product yield of the GR-AI8/GR-LI1 system progressively decreased at higher substrate concentrations.

The GR-AI9/GR-LI1 system showed a different response to increasing substrate loading (Fig. 6b). L-ribose titers of 18.80, 54.51, and 78.97 g/L were obtained from 100, 300, and 500 g/L L-arabinose, corresponding to yields of 18.80%, 18.17%, and 15.79%, respectively. Although a decrease in yield was also observed at 500 g/L substrate, the extent of this decline was markedly smaller than that observed for GR-AI8/GR-LI1. GR-AI9/GR-LI1 therefore maintained a higher product yield over the range of elevated substrate concentrations and was selected for further development on the basis of its product titer under its individually selected cell loading.

To assess the performance of the present cascade in relation to previously reported L-ribose biocatalytic systems, representative processes employing L-AIase in combination with L-ribose isomerase, mannose-6-phosphate isomerase, or D-LI were compared (Table 3) (15, 37–43). Because these studies differ substantially in enzyme combinations, catalyst formats, substrate concentrations, reaction configurations, and operating conditions, comparisons were made primarily in terms of substrate loading, L-ribose titer, and product yield rather than by direct ranking of catalytic performance.

Table 3
Comparison of representative two-enzyme or cascade systems for L-ribose production from L-arabinose

Catalytic system	Catalyst form	Initial L-arabinose	Main conditions	Time (h)	L-ribose (g/L)	Yield/conversion (%)	Reference
L-AIase + L-RIase	Free *E. coli* cells	NR	39°C, pH 8.0	NR	NR	~ 20.0	39
L-AIase + MPI	Purified enzymes	500 g/L	70°C, pH 7.0, 1 mM Co^{2+}	3	118	23.6	37
L-AIase + MPI	Immobilized co-expressing *E. coli*	300 g/L	60°C, pH 7.5, Co^{2+}	3	99	33.0	15
Sf-AI + D-LI	Sequential purified enzymes	10 mM	Sequential isomerization	16	~ 0.38	25.0	40
BlAI + BvLI	Sequential recombinant enzymes	500 g/L	50→55°C, pH 7.0, Co^{2+}/Mn^{2+}	8	105	21.0	41
L-AIase + D-LI	Co-expressing *E. coli* whole cells	500 g/L	70°C, pH 6.0, Co^{2+}	NR	50.3	10.0	38
L-AIase + L-RIase	Immobilized dual-enzyme micro-composite	NR	40°C, pH 5–6	NR	NR	22.6	42
L-AIase + L-RIase	Co-expressing *E. coli* whole cells	100 g/L	40°C, pH 8.5, 1 mM Mn^{2+}	NR	27.97	28.0	43
GR-AI9 + GR-LI1	Co-expressing *E. coli* resting cells	500 g/L	50°C, pH 7.0, 1 mM Co^{2+}	12	78.97	15.79	This study

NR, not reported. Literature values use different catalyst forms, substrate loadings, and reported yield/conversion definitions, and must not be treated as directly normalized comparisons. For this study, yield (%) = final L-ribose (g/L) / initial L-arabinose (g/L) × 100.

At an initial L-arabinose concentration of 100 g/L, GR-AI9/GR-LI1 afforded an L-ribose yield of 18.80%. This was lower than the 20.9% reported for a previously developed co-expressed L-AIase/D-LI system at the same initial substrate concentration (38) and approximately 28.0% obtained with a co-expressed L-AIase/L-ribose isomerase system (43). Patel et al. reported approximately 25.0% yield with sequential purified enzymes at a much lower L-arabinose concentration (10 mM) (40); this result is therefore not directly comparable at 100 g/L. Purified and immobilized L-AIase/mannose-6-phosphate isomerase systems have also produced reported yields of 23.6% and 33.0%, respectively, under different operating conditions (15, 37). These results do not demonstrate superior product yield of the present system relative to previously published processes.

At an initial L-arabinose concentration of 500 g/L, GR-AI9/GR-LI1 produced 78.97 g/L L-ribose with a product yield of 15.79%. These figures were higher than the 50.3 g/L and 10.0% reported for a previously described co-expressed L-AIase/D-LI whole-cell system (38), but lower than the 105 g/L and 21.0% reported for a sequential BlAI/BvLI system (41) and the 118 g/L and 23.6% reported for a purified L-AIase/mannose-6-phosphate isomerase system (37). The present measurements establish L-ribose formation at high initial substrate loading but do not independently determine substrate consumption or prove greater intrinsic catalyst activity. Furthermore, the GR-AI8/GR-LI1 and GR-AI9/GR-LI1 systems were compared at different cell loadings (20 and 40 g/L, respectively); their observed volumetric titers should not be interpreted as cell-normalized activities.

Further improvement of the cascade may require matching the catalytic capacities of the two enzyme steps and optimizing reaction conditions. Reported immobilization strategies for L-AIase/L-ribose isomerase systems (42) provide potential directions for future studies, although their effectiveness in the present GR-AI9/GR-LI1 system has not yet been examined.

4. Conclusions

Mining of the Boer goat rumen metagenome identified 79 candidate L-arabinose isomerase genes, of which nine representative genes were selected for functional characterization. Eight were successfully cloned and expressed, and GR-AI2, GR-AI6, GR-AI8, and GR-AI9 exhibited relatively high activities. GR-AI6 showed the lowest apparent Km for L-arabinose (72.99 mM), whereas GR-AI9 exhibited the highest Vmax (76.12 μmol min^{-1} mg^{-1}) and high substrate specificity. Co-expression of GR-AI8 or GR-AI9 with GR-LI1 enabled one-pot whole-cell production of L-ribose, with GR-AI9/GR-LI1 producing 78.97 g/L L-ribose from 500 g/L L-arabinose at a yield of 15.79%. These results expand the repertoire of rumen-derived L-AIases and support metagenome-guided enzyme discovery as a useful strategy for developing whole-cell L-ribose biocatalytic cascades.

Declarations

Ethics and Consent to Participate

No new animal experiments or animal sample collection were performed in the present study. The metagenomic dataset analyzed in this study was generated from previously collected goat rumen samples, as described in our previous study (34). The present study involved secondary analysis of the existing metagenomic dataset and in vitro experiments using recombinant enzymes only; therefore, no additional ethics approval or consent to participate was required.

Consent for Publication

Not applicable.

Competing Interest

The authors declare that they have no competing interests.

Author Contribution

Fengzhen Chen and Jiayun Ding performed the experiments, collected and analyzed the data, and prepared the figures. Zhanying Yang and Lulong Zhong contributed to the provision of research materials and resources. Xian'ai Shi contributed to the study design and manuscript revision. Guozeng Wang conceived and designed the study, supervised the research, coordinated the project, and revised the manuscript. All authors read and approved the final manuscript.

Funding

This work was supported by Natural Science Foundation of Fujian Province of China (2023J01408), and the Spark Project of Fujian Provincial Science and Technology Plan (2026S0052).

Availability of Data and Materials

The nucleotide sequences of the 79 L-arabinose isomerase candidate genes identified in this study have been deposited in GenBank under accession numbers QB146167–QB146245.

Acknowledgments

Not applicable.

References

1. Beerens, K., Desmet, T., & Soetaert, W. (2012). Enzymes for the biocatalytic production of rare sugars. *Journal Of Industrial Microbiology And Biotechnology*, *39*, 823–834. https://doi.org/10.1007/s10295-012-1089-x
2. Dai, D., & Jin, Y. S. (2024). Rare sugar bioproduction: advantages as sweeteners, enzymatic innovation, and fermentative frontiers. *Curr Opin Food Sci*, *56*, 101137. https://doi.org/10.1016/j.cofs.2024.101137
3. Matsuo, T., Baba, Y., Hashiguchi, M., Takeshita, K., Izumori, K., & Suzuki, H. (2001). Dietary D-psicose, a C-3 epimer of D-fructose, suppresses the activity of hepatic lipogenic enzymes in rats, Asia Pac. *J Clin Nutr*, *10*, 233–237. https://doi.org/10.1046/j.1440-6047.2001.00246.x
4. Wang, P., Hong, J. H., Cooperwood, J. S., & Chu, C. K. (1998). Recent advances in L-nucleosides: chemistry and biology. *Antiviral Research*, *40*, 19–44. https://doi.org/10.1016/S0166-3542(98)00041-2
5. Gumina, G., Song, G. Y., & Chu, C. K. (2001). L-nucleosides as chemotherapeutic agents. *Fems Microbiology Letters*, *202*, 9–15. https://doi.org/10.1111/j.1574-6968.2001.tb10773.x
6. Okano, K. (2009). Synthesis and pharmaceutical application of L-ribose, Tetrahedron 65, 1937–1949. https://doi.org/10.1016/j.tet.2008.11.047

7. Mahmood, S., Iqbal, M. W., Zhang, W., & Mu, W. (2021). A review on L-ribose isomerases for the biocatalytic production of L-ribose and L-ribulose. *Food Research International*, *145*, 110409. https://doi.org/10.1016/j.foodres.2021.110409
8. Huang, Q., Xu, Z., Li, S., et al. (2019). Advances in biomanufacturing of the pharmaceutical intermediate L-ribose. *Ind Microbiol*, *49*, 61–69. [In Chinese].
9. Ahmed, Z. (2001). Production of natural and rare pentoses using microorganisms and their enzymes. *Electronic Journal Of Biotechnology*, *4*, 103–111. https://doi.org/10.2225/vol4-issue2-fulltext-7
10. Takahashi, H., Iwai, Y., Hitomi, Y., & Ikegami, S. (2002). Novel synthesis of L-ribose from D-mannono-1,4-lactone. *Organic Letters*, *4*, 2401–2403. https://doi.org/10.1021/ol026141i
11. Qi, S., Zhang, W., & Feng, Y. (2007). Chemical synthesis of L-ribose. Nat. *Gas Chem Ind*(1), 69–71. [In Chinese].
12. Izumori, K. (2006). Izumoring: a strategy for bioproduction of all hexoses. *Journal Of Biotechnology*, *124*, 717–722. https://doi.org/10.1016/j.jbiotec.2006.04.016
13. Zhang, W., Zhang, T., Jiang, B., & Mu, W. (2017). Enzymatic approaches to rare sugar production. *Biotechnology Advances*, *35*, 267–274. https://doi.org/10.1016/j.biotechadv.2017.01.004
14. Hu, C., Li, L., Zheng, Y., Rui, L., & Hu, C. (2011). Perspectives of biotechnological production of L-ribose and its purification. *Applied Microbiology And Biotechnology*, *92*, 449–455. https://doi.org/10.1007/s00253-011-3552-4
15. Kim, K. R., Seo, E. S., & Oh, D. K. (2014). L-Ribose production from L-arabinose by immobilized recombinant *Escherichia coli* co-expressing the L-arabinose isomerase and mannose-6-phosphate isomerase genes from *Geobacillus thermodenitrificans*. *Applied Biochemistry And Biotechnology*, *172*, 275–288. https://doi.org/10.1007/s12010-013-0547-x
16. Chen, M., Wu, H., Zhang, W., & Mu, W. (2020). Microbial and enzymatic strategies for the production of L-ribose. *Applied Microbiology And Biotechnology*, *104*, 3321–3329. https://doi.org/10.1007/s00253-020-10471-9
17. Xu, Z., Li, S., Feng, X., Liang, J., & Xu, H. (2014). L-Arabinose isomerase and its use for biotechnological production of rare sugars. *Applied Microbiology And Biotechnology*, *98*, 8869–8878. https://doi.org/10.1007/s00253-014-6073-0
18. Heath, E. C., Horecker, B. L., Smyrniotis, P. Z., & Takagi, Y. (1958). Pentose fermentation by *Lactobacillus plantarum*. II. L-arabinose isomerase. *Journal Of Biological Chemistry*, *231*, 1031–1037. https://doi.org/10.1016/S0021-9258(18)70464-X
19. Salonen, N., Nyyssölä, A., Salonen, K., & Turunen, O. (2012). *Bifidobacterium longum* L-arabinose isomerase—overexpression in *Lactococcus lactis*, purification, and characterization. *Applied Biochemistry And Biotechnology*, *168*, 392–405. https://doi.org/10.1007/s12010-012-9783-8
20. Chouayekh, H., Bejar, W., Rhimi, M., Jelleli, K., Mseddi, M., & Bejar, S. (2007). Characterization of an L-arabinose isomerase from the *Lactobacillus plantarum* NC8 strain showing pronounced stability at acidic pH. *Fems Microbiology Letters*, *277*, 260–267. https://doi.org/10.1111/j.1574-6968.2007.00961.x
21. Rhimi, M., Ilhammami, R., Bajic, G., Boudebbouze, S., Maguin, E., Haser, R., & Aghajari, N. (2010). The acid tolerant L-arabinose isomerase from the food grade *Lactobacillus sakei* 23K is an attractive D-tagatose producer. *Bioresource Technology*, *101*, 9171–9177. https://doi.org/10.1016/j.biortech.2010.07.036

22. Staudigl, P., Haltrich, D., & Peterbauer, C. K. (2014). L-Arabinose isomerase and D-xylose isomerase from *Lactobacillus reuteri*: characterization, coexpression in the food grade host *Lactobacillus plantarum*, and application in the conversion of D-galactose and D-glucose. *Journal Of Agriculture And Food Chemistry*, *62*, 1617–1624. https://doi.org/10.1021/jf404785m
23. Zhang, H., Jiang, B., & Pan, B. (2007). Purification and characterization of L-arabinose isomerase from *Lactobacillus plantarum* producing D-tagatose. *World Journal Of Microbiology & Biotechnology*, *23*, 641–646. https://doi.org/10.1007/s11274-006-9274-6
24. Nirwantono, R., Laksmi, F. A., Nuryana, I., Firdausa, S., Herawan, D., Giyandini, R., & Hidayat, A. A. (2024). Exploring an L-arabinose isomerase from cryophile bacteria *Arthrobacter psychrolactophilus* B7 for D-tagatose production. *International Journal Of Biological Macromolecules*, *254*, 127781. https://doi.org/10.1016/j.ijbiomac.2023.127781
25. Souza, A. G. V., Pepe, E. S. G., Pereira, P. A. M., Castellane, T. C. L., & Lemos, E. G. M. (2025). Biochemical characterization of a novel arabinose isomerase for rare sugar production and optimization through enzyme immobilization. *International Journal Of Biological Macromolecules*, *319*, 145521. https://doi.org/10.1016/j.ijbiomac.2025.145521
26. Ariaeenejad, S., Gharechahi, J., Foroozandeh Shahraki, M., Fallah Atanaki, F., Han, J. L., Ding, X. Z., Hildebrand, F., Bahram, M., Kavousi, K., & Hosseini Salekdeh, G. (2024). Precision enzyme discovery through targeted mining of metagenomic data. *Nat Prod Bioprospect*, *14*, 7. https://doi.org/10.1007/s13659-023-00426-8
27. Robinson, S. L., Piel, J., & Sunagawa, S. (2021). A roadmap for metagenomic enzyme discovery. *Natural Products Reports*, *38*, 1994–2023. https://doi.org/10.1039/d1np00006c
28. Prayogo, F. A., Budiharjo, A., Kusumaningrum, H. P., Wijanarka, W., Suprihadi, A., & Nurhayati, N. (2020). Metagenomic applications in exploration and development of novel enzymes from nature: a review. *J Genet Eng Biotechnol*, *18*, 39. https://doi.org/10.1186/s43141-020-00043-9
29. de Souza Colombo, G., Viana Mendes, I., de Morais Souto, B., Barreto, C. C., Serra, L. A., Noronha, E. F., Parachin, N. S., de Almeida, J. R. M., & Quirino, B. F. (2022). Identification and functional expression of a new xylose isomerase from the goat rumen microbiome in *Saccharomyces cerevisiae*. *Letters In Applied Microbiology*, *74*, 941–948. https://doi.org/10.1111/lam.13689
30. Hou, J., Shen, Y., Jiao, C., Ge, R., Zhang, X., & Bao, X. (2016). Characterization and evolution of xylose isomerase screened from the bovine rumen metagenome in *Saccharomyces cerevisiae*. *Journal Of Bioscience And Bioengineering*, *121*, 160–165. https://doi.org/10.1016/j.jbiosc.2015.05.014
31. Madhavan, A., Tamalampudi, S., Ushida, K., Kanai, D., Katahira, S., Srivastava, A., Fukuda, H., Bisaria, V. S., & Kondo, A. (2009). Xylose isomerase from polycentric fungus Orpinomyces: gene sequencing, cloning, and expression in *Saccharomyces cerevisiae* for bioconversion of xylose to ethanol. *Applied Microbiology And Biotechnology*, *82*, 1067–1078. https://doi.org/10.1007/s00253-008-1794-6
32. Liu, X., Li, H., Ke, Y., Zhang, K., Li, X., Li, X., Fu, J., & Li, H. (2017). Cloning and expression of the linoleic acid isomerase gene of *Lactobacillus casei* isolated from cattle rumen. *Food Sci*, *38*, 1–5. https://doi.org/10.7506/spkx1002-6630-201706001
33. Zhang, S., Ma, R., Shi, P., Huang, H., & Xu, B. (2015). Preliminary studies on genetic diversity of L-arabinose isomerase in sheep rumen bacteria. *J Agric Sci Technol*, *17*, 95–101. https://doi.org/10.13304/j.nykjdb.2014.190. [In Chinese].

34. Xu, X., Chen, M., Su, Y., Ding, J., Xie, X., Zhang, X., Li, F., Shi, X., & Wang, G. (2025). Identification and characterization of novel D-lyxose isomerases from the goat rumen metagenome. *Process Biochemistry*, *149*, 213–221. https://doi.org/10.1016/j.procbio.2024.12.014
35. Bradford, M. M. (1976). A rapid and sensitive method for the quantitation of microgram quantities of protein utilizing the principle of protein-dye binding. *Analytical Biochemistry*, *72*, 248–254. https://doi.org/10.1016/0003-2697(76)90527-3
36. Dische, Z., & Borenfreund, E. (1951). A new spectrophotometric method for the detection and determination of keto sugars and trioses. *Journal Of Biological Chemistry*, *192*, 583–587. https://doi.org/10.1016/S0021-9258(19)77782-5
37. Yeom, S. J., Kim, N. H., Park, C. S., & Oh, D. K. (2009). L-Ribose production from L-arabinose by using purified L-arabinose isomerase and mannose-6-phosphate isomerase from *Geobacillus thermodenitrificans*. *Applied And Environment Microbiology*, *75*, 6941–6943. https://doi.org/10.1128/AEM.01867-09
38. Wu, H., Huang, J., Deng, Y., Zhang, W., & Mu, W. (2020). Production of L-ribose from L-arabinose by co-expression of L-arabinose isomerase and D-lyxose isomerase in *Escherichia coli*. *Enyzme And Microbial Technology*, *132*, 109443. https://doi.org/10.1016/j.enzmictec.2019.109443
39. Helanto, M., Kiviharju, K., Granström, T., Leisola, M., & Nyyssölä, A. (2009). Biotechnological production of L-ribose from L-arabinose. *Applied Microbiology And Biotechnology*, *83*, 77–83. https://doi.org/10.1007/s00253-008-1855-x
40. Patel, M. J., Akhani, R. C., Patel, A. T., Dedania, S. R., & Patel, D. H. (2017). A single and two step isomerization process for D-tagatose and L-ribose bioproduction using L-arabinose isomerase and D-lyxose isomerase. *Enyzme And Microbial Technology*, *97*, 27–33. https://doi.org/10.1016/j.enzmictec.2016.11.001
41. Guo, Z., Long, L., & Ding, S. (2019). Characterization of a D-lyxose isomerase from *Bacillus velezensis* and its application for the production of D-mannose and L-ribose. *AMB Express*, *9*, 149. https://doi.org/10.1186/s13568-019-0877-3
42. Singh, A., Rai, S. K., & Yadav, S. K. (2022). Metal-based micro-composite of L-arabinose isomerase and L-ribose isomerase for the sustainable synthesis of L-ribose and D-talose, Colloids Surf. *B Biointerfaces*, *217*, 112637. https://doi.org/10.1016/j.colsurfb.2022.112637
43. Mahmood, S., Iqbal, M. W., Arsalan, A., Tang, X., Ravikumar, Y., Zhao, M., Zhang, C., & Qi, X. (2025). Harnessing co-expressed L-arabinose and L-ribose isomerases to enhance the biosynthesis of L-ribose. *Biochemical Engineering Journal*, *215*, 109594. https://doi.org/10.1016/j.bej.2024.109594

Figures

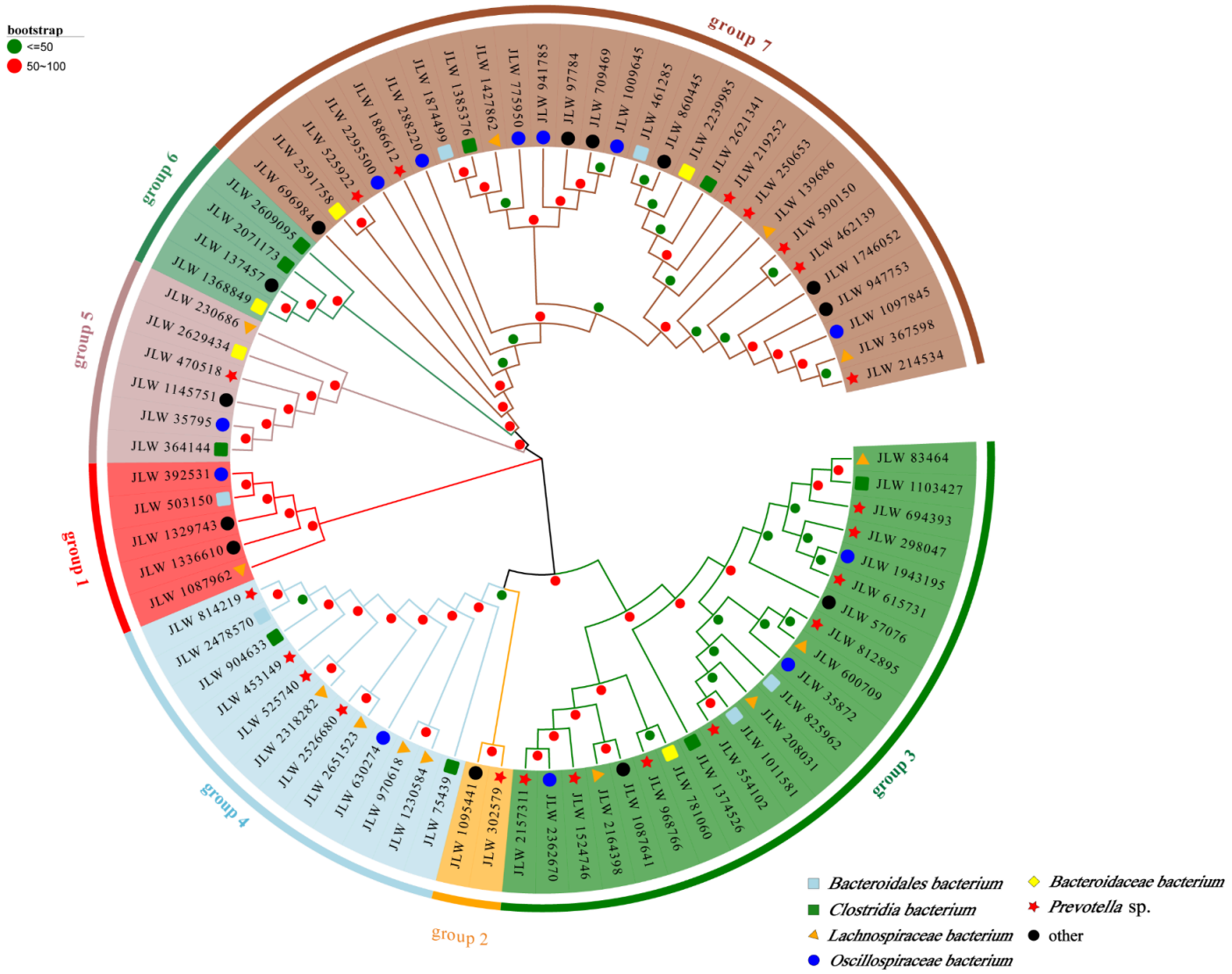

Figure 1

Phylogenetic analysis of putative L-arabinose isomerases identified from the goat rumen metagenome. A total of 79 candidate sequences were classified into seven phylogenetic groups (Groups 1–7), indicated by different background colors. Symbols at the branch tips represent the putative taxonomic affiliations of the corresponding sequences, as indicated in the legend. Bootstrap support values are represented by colored circles at the internal nodes (green, ≤50%; red, >50%).

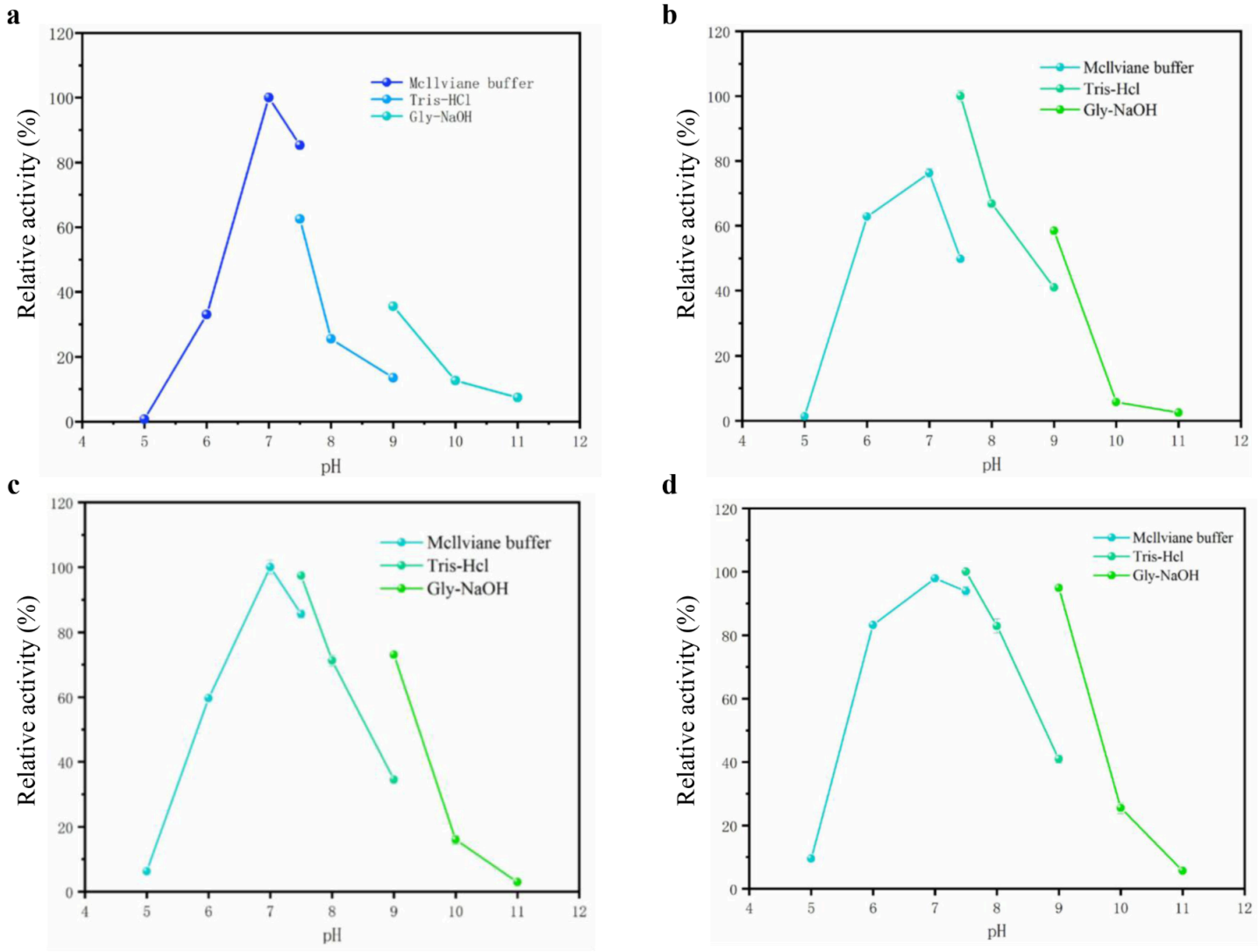

Figure 2

Effects of pH on the activities of four recombinant L-AIases. (a) GR-AI2; (b) GR-AI6; (c) GR-AI8; and (d) GR-AI9. Enzyme activities were measured at different pH values using McIlvaine, Tris-HCl, and glycine-NaOH buffers. The highest activity of each enzyme was defined as 100%, and the activities at other pH values were expressed as relative activities.

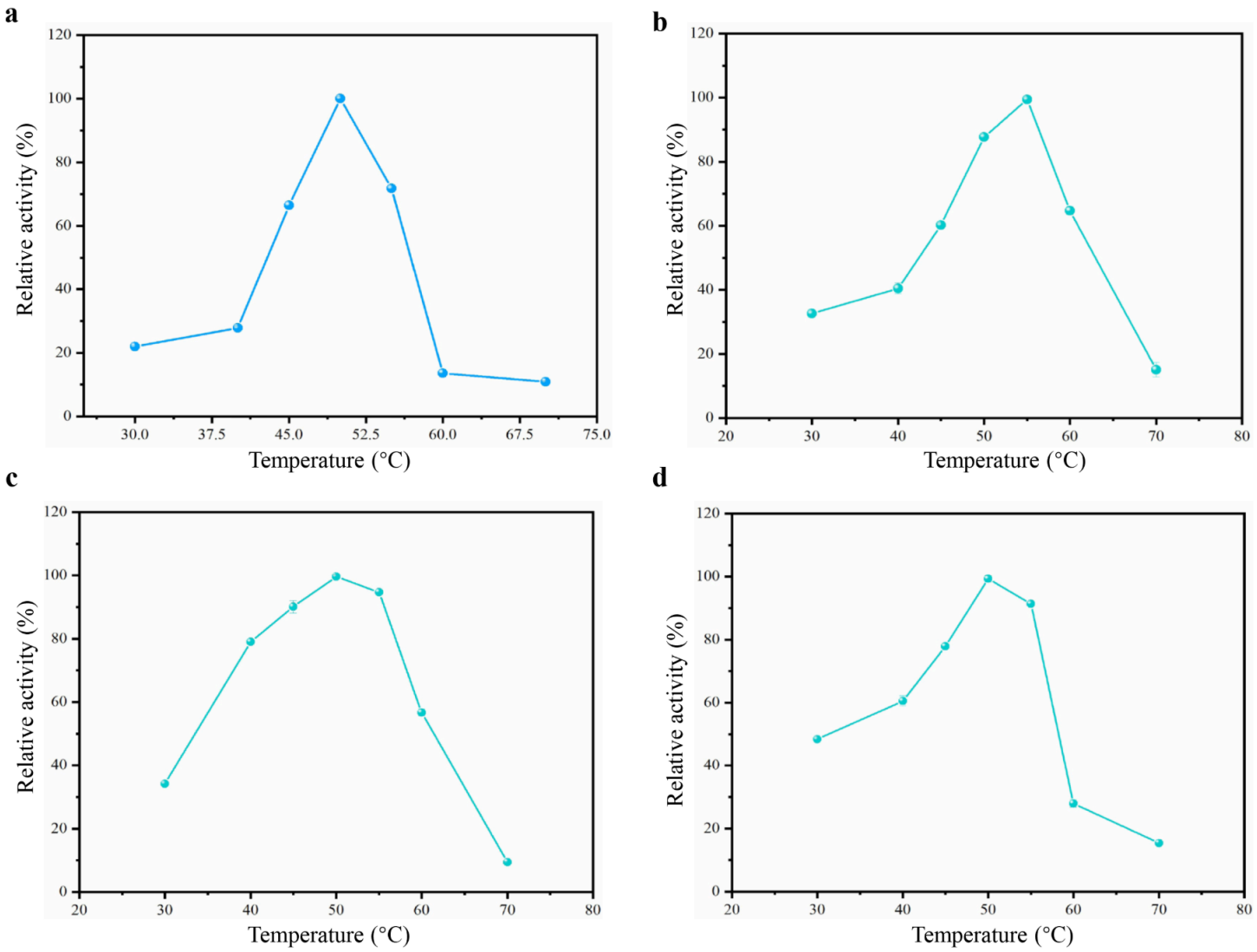

Figure 3

Effects of temperature on the activities of four recombinant L-AIases. (a) GR-AI2; (b) GR-AI6; (c) GR-AI8; and (d) GR-AI9. Enzyme activities were measured at different temperatures (30–70 °C). The highest activity of each enzyme was defined as 100%, and the activities at other temperatures were expressed as relative activities.

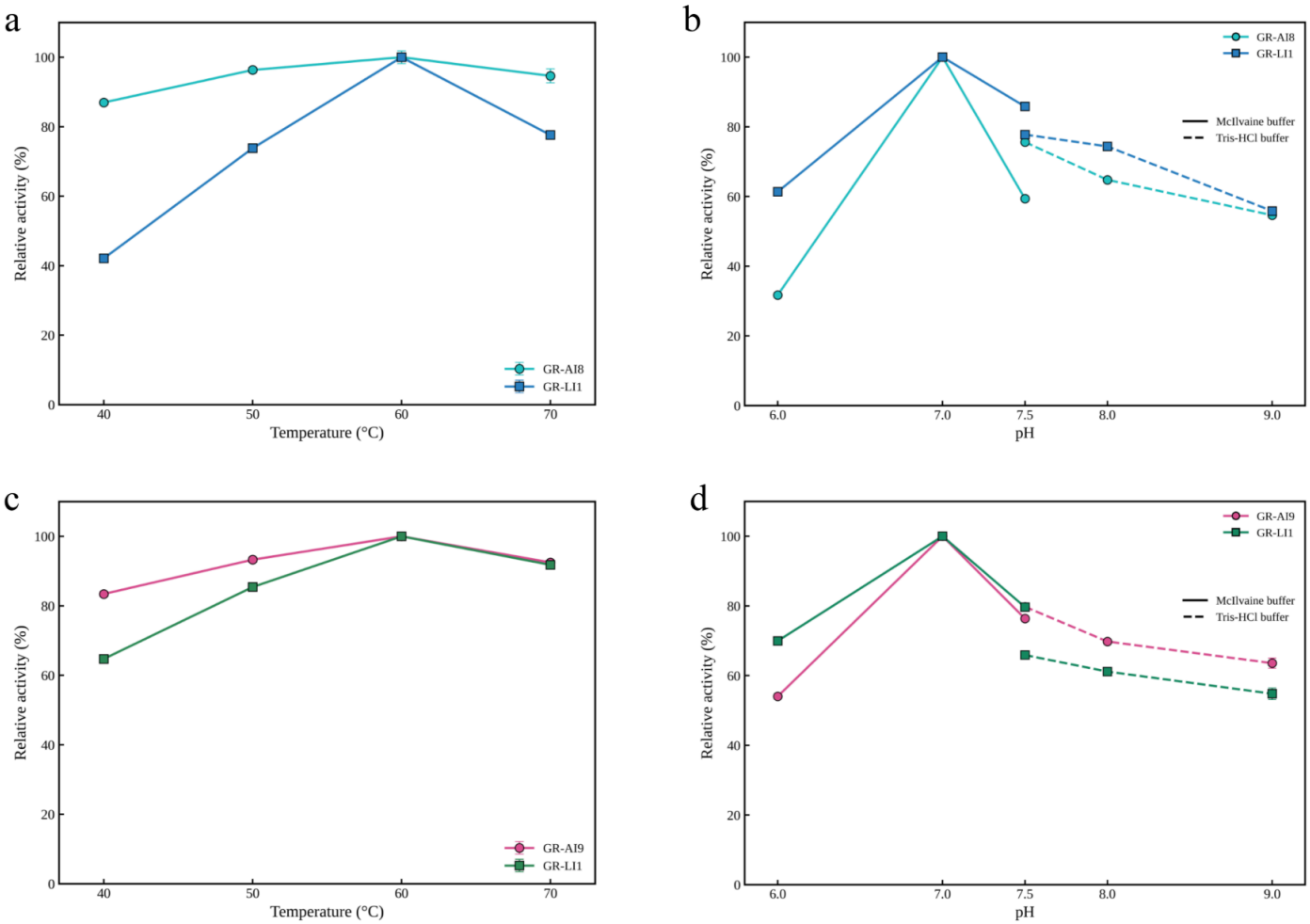

Figure 4

Effects of temperature and pH on the relative activities of enzymes in the co-expression systems. (a, b) Temperature and pH profiles of the GR-AI8/GR-LI1 co-expression system, respectively. (c, d) Temperature and pH profiles of the GR-AI9/GR-LI1 co-expression system, respectively. Relative activities are expressed as percentages of the maximum activity.

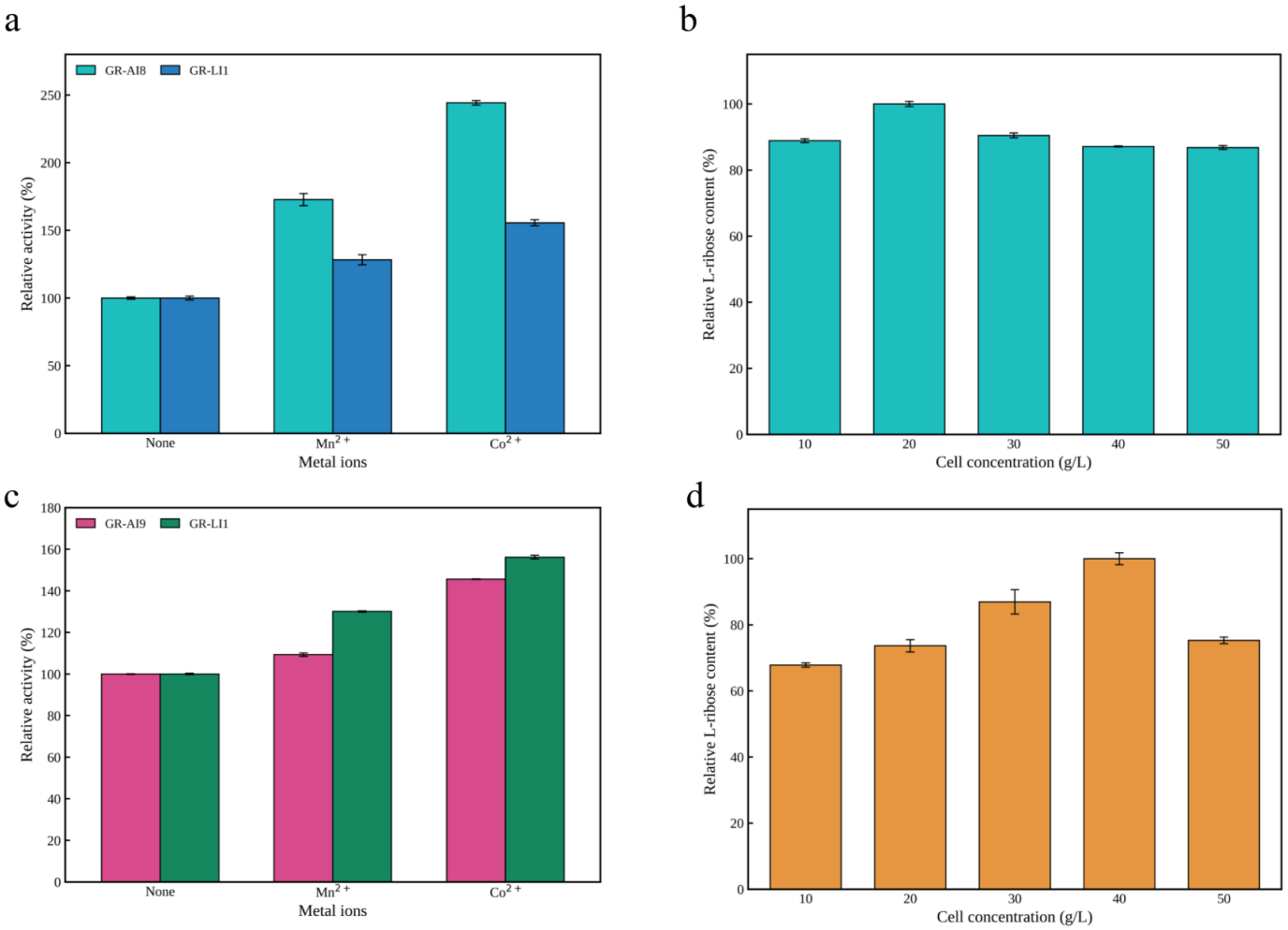

Figure 5

Effects of metal ions and resting-cell concentration on the co-expression systems. (a) Effects of metal ions (Mn^{2+} and Co^{2+}) on the relative activities of GR-AI8 and GR-LI1. (b) Effect of resting-cell concentration on the relative L-ribose production in the GR-AI8/GR-LI1 co-expression system. (c) Effects of metal ions (Mn^{2+} and Co^{2+}) on the relative activities of GR-AI9 and GR-LI1. (d) Effect of resting-cell concentration on the relative L-ribose production in the GR-AI9/GR-LI1 co-expression system.

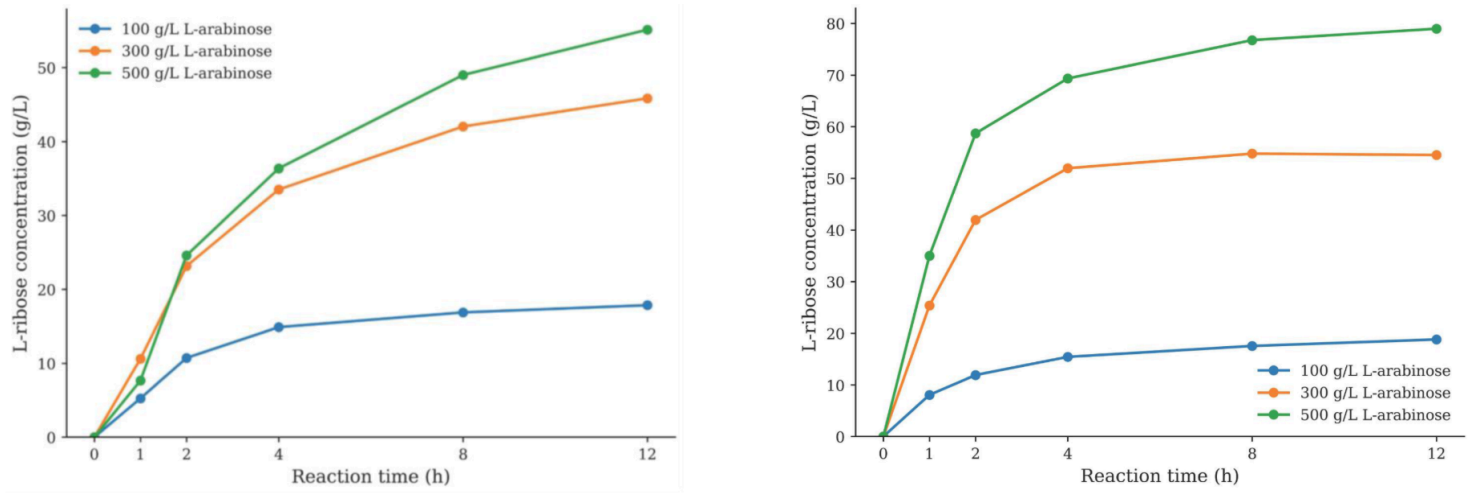

Figure 6

Time courses of L-ribose production by whole-cell biocatalysts at different initial L-arabinose concentrations. (a) L-ribose production by the GR-AI8/GR-LI1 co-expression system. (b) L-ribose production by the GR-AI9/GR-LI1 co-expression system. The initial L-arabinose concentrations were 100, 300, and 500 g/L. L-Ribose concentrations were monitored over a 12-h reaction period.

Supplementary Files

This is a list of supplementary files associated with this preprint. Click to download.

- SupplementaryInformation.docx